Amino Acids (2004) 27: 129–140
DOI 10.1007/s00726-004-0125-1

Amino Acids
Printed in Austria

Expression of proteasomal proteins in ten different tumor cell lines

L. Afjehi-Sadat, M. Gruber-Olipitz, M. Felizardo, I. Slavc, and **G. Lubec**

Division of Basic Sciences, Department of Pediatrics, Medical University of Vienna, Vienna, Austria

Received May 3, 2004
Accepted August 10, 2004
Published online October 4, 2004; © Springer-Verlag 2004

Summary. Controlled intracellular protein degradation is crucial for the maintenance of normal cell functions. An evolving concept claims that alterations in the exact timely degradation of proteins involved in growth control, apoptosis, signaling and differentiation contribute to carcinogenesis. This tightly regulated process is facilitated by the ubiquitin-26S proteasome system, a multi-enzyme complex, and inhibitors of this pathway have already been developed as potential anticancer agents.

In order to generate proteasomal protein expression patterns of tumor cells and to provide an analytical tool we applied two-dimensional electrophoresis (2-DE) followed by mass spectrometry (MALDI-TOF-TOF with LIFT technology) in ten individual tumor cell lines (Saos-2; SK-N-SH; HCT-116; Caov3; A-549; HL60; A-673; A-375; MCF-7; HeLa) widely used in tumor research. A series of 39 proteasomal/proteolytic proteins was unambiguously identified by this proteomic approach, comprising proteins of the 20S core complex, the 19S regulatory complex, the 11S regulator, components of the ubiquitin pathway and proteases.

Construction of individual protein maps by 2-DE and mass spectrometry provides an analytical tool and reference base for studying the pivotal importance of the proteasome and other proteolytic enzymes in tumor cells, independent of antibody availability and specificity. This preliminary database enables for designing studies in this area of research and reveals proteins that can be used as targets for new therapeutic strategies.

Keywords: Proteasome – Tumor cell line – Cancer – Protein profiling

1 Introduction

Development and maintenance of malignant features in cancer cells is characterized by deregulated protein synthesis involved in different cellular pathways including those of growth control, apoptosis, signaling and differentiation. Moreover, alteration of timely degradation of proteins from these cascades becomes an evolving concept in carcinogenesis.

Intracellular protein degradation is a highly selective and tightly regulated process. The vast majority of proteolytic activity is facilitated by the 26S proteasome complex consisting of a catalytic central 20S core and a regulatory 19S cap complex, present in both, cytoplasm and nucleus. Proteins determined for degradation need a special labeling with polyubiquitin chains to be recognized by the proteasome complex. This so-called ubiquitination is mediated by a complex cascade of enzymes comprising ubiquitin activating enzymes, conjugating enzymes and ligases (Doherty et al., 2002; Ohta and Fukuda, 2004; Sakamoto, 2002).

Among the many substrates of the proteasome complex, proteins involved in cell cycle and apoptotic pathways are of special interest as their impact on carcinogenesis is enormous (Adams, 2004; Jesenberger and Jentsch, 2002).

Cyclins, e.g., represent a group of proteins regulating cell cycle progression by modulating cyclin-dependent kinase activities. Their distinct function in different phases of the cell cycle is mandatory and is achieved by rapid degradation of kinases throughout each cell cycle phase and a highly active and properly working ubiquitin-proteasome pathway is mandatory for proliferating cells whereas inhibition of the proteasome complex retards cell growth (Glotzer et al., 1991).

In addition, the ubiquitin-proteasome pathway plays a crucial role in the regulation of programmed cell death, because regulatory molecules as well as key enzymes of apoptosis have been identified as proteasomal substrates.

In normal cells, the tumor-suppressor protein p53 is rapidly degraded by the ubiquitin-proteasome pathway; ubiquitination is carried out by ubiquitin-ligase MDM2, which also inhibits transcriptional activity of p53. However, in response to cellular stresses ubiquitination is inhibited, p53 accumulates leading to cell-cycle arrest, DNA repair and apoptosis (Jesenberger and Jentsch, 2002; Yang et al., 2004; Chene, 2003).

In numerous cancer cell lines deficient p53 function – mainly resulting from p53 mutations – is leading to inhibition of apoptosis. p53 deficiency, however, may be due to overexpression of MDM2 as well, resulting into increased degradation of the protein by the proteasome complex (Yang et al., 2004).

Another link between the ubiquitin-proteasome pathway and apoptosis is reflected by the activation of NF-kB by the proteasome complex due to degradation of the NF-kB inhibitor IkB: Active NF-kB leads to specific growth advantages of the cell by directing the transcription of growth factors, angiogenetic and anti-apoptotic factors (Adams, 2004; Jesenberger and Jentsch, 2002). And indeed, constitutive activation of NF-kB is found in many tumor types paralleling the decrease of susceptibility to chemotherapeutic agents and mediating drug resistance (Karin et al., 2002). Inhibition of the proteasome by N-acetyl-L-leucinyl-L-leucinyl-L-norleucinal (Jeremias et al., 1998) and thus prevention of NF-kB activation not only helps to overcome resistance by sensitizing cells to chemotherapy (Cusack et al., 2001; Wang et al., 1999) but may directly induce apoptosis in cancer cells.

Among others, one mechanism is that caspases, enzymes that execute apoptosis through a complex process of cell disintegration, are inactivated by NF-kB (Adams, 2004) i.e. deactivation of NF-kB is potentiating caspase activity.

Different substance classes were empirically found to inhibit the proteasome complex, preferentially in actively proliferating malignant cells thereby enhancing apoptosis in various cancer cells (Adams, 2004).

A putative mechanism of this differential susceptibility of malignant versus normal cells might be that highly proliferating cells rely much more on removal of aberrant proteins to evade apoptosis. Another explanation might be that some cancer cells rely on the proteasome dependent NF-kB activation to evade apoptosis and maintain drug or radiation resistance (Karin et al., 2002).

Bortezomib (PS-341) is a proteasome inhibitor already in clinical use for therapy of relapsing multiple myeloma and additional compounds are currently under investigation in preclinical settings to reveal the precise mechanism of the many encounters between the ubiquitin-proteasome pathways and apoptosis. Bypassing drug resistance by the combination of proteasome inhibition along with conventional chemotherapy seems to be a promising therapeutic strategy (Adams, 2004).

Involvement of the proteasome in different pathways important for tumor biology as well as the availability of specific inhibitors for cancer treatment formed the rationale for the present study. The major aim was to generate a map of proteasomal proteins as well as associated regulatory and activating enzymes, in a variety of tumor cells widely used in tumor research. We intended to generate protein expressional patterns by a high-throughput proteomic approach, a protein chemical rather than an immunochemical method, independent of antibody availability or specificity allowing the concomitant reliable determination of proteins. Moreover, we decided to provide an analytical tool for the creation of a proteasomal reference database and maps in tumor cell lines.

A series of abundant proteasome proteins and associated proteolytic enzymes forming the basis for expressional studies on tumor cells and tissues at the protein rather than at the nucleic acid level were identified, as there is a long and unpredictable way from RNA to protein and it is the protein that finally carries out function.

2 Material and methods

2.1 Cell culture

Ten different tumor cell lines were purchased from American Type Culture Collection (ATCC). The cell lines and their ATCC no. are given in Table 1.

SK-N-SH and HeLa cervix cell lines were cultured in Minimum Essential Medium (Eagle) with 2 mM L-glutamine and Earle's Basic Salt Solution (BSS) adjusted to contain 1.5 g/L sodium bicarbonate, 0.1 mM non-essential amino acids, and 1.0 mM sodium pyruvate, with 10% fetal bovine serum (FBS). The same conditions were used to culture MCF-7 cell line except for supplementing 10% FBS with 90% 0.01 mg/ml bovine insulin. Saos-2 cell line was cultured in McCoy's 5a medium with 90% 1.5 mM L-glutamine and 10% FBS. The A-549 cell line was cultured with Ham's F12K medium with 2 mM L-glutamine adjusted to contain 1.5 g/L sodium bicarbonate and 10% FBS. HL-60 cell line was cultured with Iscove's modified Dulbecco's medium with 4 mM L-glutamine adjusted to contain 80% 1.5 g/L sodium bicarbonate and 20% FBS. A-673 and A-375 cell lines were cultured in DMEM with 4 mM L-glutamine adjusted to contain 1.5 g/L sodium bicarbonate and 4.5 g/L glucose with 10% FBS.

Table 1. Identification of investigated cell lines (ATCC)

Name	ATCC no.	Cancer type	Source
Saos-2	HTB-85	Osteosarcoma	Bone
SK-N-SH	HTB-11	Neuroblastoma	Brain
HCT-116	CCL-247	Colorectal carcinoma	Colon
Caov3	HTB-75	Adenocarcinoma	Ovary
A-549	CCL-185	Carcinoma	Lung
HL-60	CCL-240	Leukemia (promyelocytic)	Peripheral blood
A-673	CRL-1598	Rhabdomyosarcoma	Muscle
A-375	CRL-1619	Malignant melanoma	Skin
MCF-7	HTB-22	Adenocarcinoma	Mammary gland
Hela	CCL-2	Adenocarcinoma	cervix

Cell cultures were maintained in a humidified atmosphere of 5% v/v CO_2 in air at 37°C.

2.2 Sample preparation

Harvested cells were washed three times with 10 mL PBS (phosphate buffered saline) (Gibco BRL, Gaithersburg, MD, USA) and centrifuged for 10 min at 800 g at room temperature. The supernatant was discarded and the pellet was suspended in 1.0 ml of sample buffer consisting of 7 M urea (Merck, Darmstadt, Germany), 2 M thiourea (Sigma, St. Louis, MO, USA), 4% CHAPS (3-[(3-cholamidopropyl) dimethylammonio]-1-propane-sulfonate) (Sigma, St. Louis, MO, USA), 65 mM 1,4-dithioerythritol (Merck, Germany), 1 mM EDTA (ethylenediaminetraacetic acid) (Merck, Germany), protease inhibitors complete® (Roche, Basel, Switzerland) and 1 mM phenylmethylsulfonyl chloride. The suspension was sonicated for approximately 15 sec. After homogenisation samples were left at room temperature for 1 h and centrifuged at 14,000 rpm for 1 h. The supernatant was transferred into Ultrafree-4 centrifugal filter unit (Millipore, Bedford, MA), for desalting and concentrating proteins. Protein content of the supernatant was quantified by Bradford protein assay system (Bradford, 1976). The standard curve was generated using bovine serum albumin and absorbance was measured at 595 nm.

2.3 Two-dimensional gel electrophoresis (2-DE)

Samples prepared from each cell line were subjected to 2-DE as described elsewhere (Weitzdoerfer et al., 2002).

1 mg protein was applied on immobilized pH 3–10 nonlinear gradient strips in sample cups at their basic and acidic ends. Focusing was started at 200 V and the voltage was gradually increased to 5000 V at a rate of 3 V/min and then kept constant for a further 24 h (approximately 180,000 Vh totally). After the first dimension, strips (13 cm) were equilibrated for 15 min in the buffer containing 6 M urea, 20% glycerol, 2% SDS, 2% DTT and then for 15 min in the same buffer containing 2.5% iodo-acetamide instead of DDT. After equilibration, strips were loaded on 9–16% gradient sodium dodecylsulfate polyacrylamide gels for second-dimensional separation. Gels ($180 \times 200 \times 1.5$ mm) were run at 40 mA per gel. Immediately after the second dimension run gels were fixed for 18 h in 50% methanol, containing 10% acetic acid, gels were stained with Colloidal Coomassie Blue (Novex, San Diego, CA) for 12 h on a rocking shaker. Molecular masses were determined by running standard protein markers (Biorad Laboratories, Hercules, CA) covering the range 10–250 kDa. pI values 3–10 were used as given by the supplier of the immobilized pH gradient strips (Amersham Bioscience, Uppsala, Sweden). Excess of dye was washed out from the gels with distilled water and the gels were scanned with ImageScanner (Amersham Bioscience).

Electronic images of the gels were recorded using Adobe Photoshop and Microsoft Power Point Softwares.

2.4 Matrix-assisted laser desorption ionisation mass spectrometry

Spots were excised with a spot picker (PROTEINEER sp™, Bruker Daltonics, Bremen, Germany), placed into 96-well microtiter plates and in-gel digestion and sample preparation for MALDI analysis were performed by an automated procedure (PROTEINEER dp™, Bruker Daltonics) (Suckau et al., 2003; Yang et al., 2004). Briefly, spots were excised and washed with 10 mM ammonium bicarbonate and 50% acetonitrile in 10 mM ammonium bicarbonate. After washing, gel plugs were shrunk by addition of acetonitrile and dried by blowing out the liquid through the pierced well bottom. The dried gel pieces were reswollen with 40 ng/μl trypsin (Roche Diagnostics, Penzberg, Germany) in enzyme buffer (consisting of 5 mM Octyl β-D-glucopyranoside (OGP) and 10 mM ammonium bicarbonate) and incubated for 4 hrs at 30°C. Peptide extraction was performed with 10 μl of 1% TFA in 5 mM OGP. Extracted peptides were directly applied onto a target (AnchorChip™, Bruker Daltonics) that was load with α-cyano-4-hydroxy-cinnamic acid (Bruker Daltonics) matrix thinlayer. The mass spectrometer used in this work was an Ultraflex™ TOF/TOF (Bruker Daltonics) operated in the reflector mode for MALDI-TOF peptide mass fingerprint (PMF) or LIFT mode for MALDI-TOF/TOF with a fully automated mode using the FlexControl™ software. An accelerating voltage of 25 kV was used for PMF. Calibration of the instrument was performed externally with $[M+H]^+$ ions of angiotensin I, angiotensin II, substance P, bombesin, and adrenocorticotropic hormones (clip 1–17 and clip 18–39). Each spectrum was produced by accumulating data from 200 consecutive laser shots. Those samples which were analyzed by PMF from MALDI-TOF were additionally analyzed using LIFT-TOF/TOF MS/MS from the same target. A maximum of three precursor ions per sample were chosen for MS/MS analysis. In the TOF1 stage, all ions were accelerated to 8 kV under conditions promoting metastable fragmentation. After selection of jointly migrating parent and fragment ions in a timed ion gate, ions were lifted by 19 kV to high potential energy in the LIFT cell. After further acceleration of the fragment ions in the second ion source, their masses could be simultaneously analyzed in the reflector with high sensitivity. PMF and LIFT spectra were interpreted with the Mascot software (Matrix Science Ltd, London, UK). Database searches, through Mascot, using combined PMF and MS/MS datasets were performed via BioTools 2.2 software (Bruker). A mass tolerance of 100 ppm and 2 missing cleavage sites for PMF and MS/MS tolerance of 0.5 Da and 1 missing cleavage sites for MS/MS search were allowed and oxidation of methionine residues was considered. The probability score calculated by the software was basically used as criterion for correct identification.

The algorithm used for determining the probability of a false positive match with a given mass spectrum is described elsewhere (Berndt et al., 1999).

3 Results and discussion

A series of 28 high abundance proteasomal proteins and 11 proteolytic enzymes was identified and a preliminary reference database and cell line-specific expressional pattern was generated. Table 2 presents the list of proteins describing Swissprot Accession number, protein name, cell lines in which proteins were detected, theoretical and observed pI, theoretical and observed molecular weight as well as peptides matched and Mascot scores. Protein maps revealing the individual expressional patterns are given in Figs. 1–10.

Individual and representative proteins from the 26S proteasome/ubiquitin complex were analysed and grouped into the 20S core, the 19S regulatory complex, the 11S regulator and ubiquitin pathway components.

The 20S core, a cylindric ring-forming structure consisting of alpha- and beta subunits carrying out proteolytic degradation, was represented by 9 proteins, proteasome subunit alpha type 1, 2, 3, 4, 7 and proteasome subunit beta type 1, 2, 3, 4. Except proteasome subunit beta type 2 and 3 with two expression forms each, all 20S core components were represented by a single spot. Observed pIs were corresponding to predicted pI values (Table 2).

Table 2. Proteasomal protein expression of ten different tumor cell lines (TMW = theoretical molecular weight)

Cell line	Molecular weight	Observed pI	Peptides matched	Scores
20S core complex				
P25786	Proteasome subunit alpha type 1		Theoretical pI = 6.15	TMW = 29555
HL-60	29822	6.5	17	87
HCT116	29822	6.5	12	89
Hela cervix	29822	6.6	29	226
P25787	Proteasome subunit alpha type 2		Theoretical pI = 7.12	TMW = 25767
Saos-2	25865	6.9	14	104
A_549	25865	6.6	13	118
Hela cervix	25865	6.7	12	81
P25788	Proteasome subunit alpha type 3		Theoretical pI = 5.19	TMW = 28302
HL-60	27858	5.2	21	168
A-375	27858	5.2	19	129
A_673	27858	5.7	13	98
MCF-7	28512	5.3	19	134
Hela cervix	27858	5.2	20	142
P25789	Proteasome subunit alpha type 4		Theoretical pI = 7.58	TMW = 29484
HL-60	29750	7.2	14	82
Hela cervix	22290	7.4	14	97
O14818	Proteasome subunit alpha type 7		Theoretical pI = 8.60	TMW = 27887
A_549	28057	8.1	14	91
P20618	Proteasome subunit beta type 1		Theoretical pI = 8.27	TMW = 26489
SK_N_SH	26674	8.4	13	93
P49721	Proteasome subunit beta type 2		Theoretical pI = 6.52	TMW = 22836
Saos-2	22993	6.7	7	70
A_673	22993	6.7	10	82
	40264	5.8	22	155
MCF-7	22993	6.7	17	142
P49720	Proteasome subunit beta type 3		Theoretical pI = 6.14	TMW = 22949
A_549	23219	5.9	14	155
	22993	6.5	11	102
MCF-7	23201	6.2	15	113
Hela cervix	23219	6.3	16	116
P28070	Proteasome subunit beta type 4 (precursor)		Theoretical pI = 5.72	TMW = 29192
HL-60	29243	5.7	12	67
A-375	29230	5.7	19	113
A_673	29230	5.7	17	101
Hela cervix	29230	5.7	18	93
11S regulator				
Q06323	Proteasome activator complex subunit 1		Theoretical pI = 5.78	TMW = 28723
A_549	28876	5.6	20	165
A-375	28876	5.8	18	136
Hela cervix	28876	5.8	26	216
Q12920	Proteasome activator complex subunit 3		Theoretical pI = 5.69	TMW = 29506
A_549	29602	5.6	24	208

(*continued*)

Table 2 (*continued*)

Cell line	Molecular weight	Observed pI	Peptides matched	Scores
19S regulatory complex				
P62191	26S protease regulatory subunit 4		Theoretical pI = 5.87	TMW = 49184
SK_N_SH	49325	5.9	20	103
MCF-7	49325	5.9	27	238
P17980	26S protease regulatory subunit 6A		Theoretical pI = 5.13	TMW = 49203
HL-60	49458	5.3	33	217
A-375	49458	5.2	47	309
A_673	49458	5.3	24	165
MCF-7	49458	5.4	26	183
Hela cervix	49458	5.3	36	235
P43686	26S protease regulatory subunit 6B		Theoretical pI = 5.09	TMW = 47366
Saos-2	47451	5.2	20	136
HCT116	47451	5.2	21	125
A_549	47451	5.1	16	91
A_673	47451	5.2	21	129
P35998	26S protease regulatory subunit 7		Theoretical pI = 5.72	TMW = 48502
Saos-2	49002	5.8	33	210
SK_N_SH	49002	5.8	30	189
HCT116	49002	5.8	31	199
CaOva3	49002	5.8	25	139
P62195	26S protease regulatory subunit 8		Theoretical pI = 7.11	TMW = 45626
HL-60	45795	7.4	23	145
A_673	45795	7.0	28	178
MCF-7	45768	7.0	17	108
P62333	26S protease regulatory subunit S10B		Theoretical pI = 7.09	TMW = 44173
A-375	44418	7.45	28	202
O75832	26S proteasome non-ATPase regulatory subunit 10		Theoretical pI = 5.71	TMW = 24428
Hela cervix	24697	5.8	12	79
O00231	26S proteasome non-ATPase regulatory subunit 11		Theoretical pI = 6.08	TMW = 47463
MCF-7	47719	6.2	36	281
Q9UNM6	26S proteasome non-ATPase regulatory subunit 13		Theoretical pI = 5.53	TMW = 42918
SK_N_SH	43176	5.7	21	96
A_549	43176	5.5	15	93
MCF-7	43203	5.7	26	176
O00487	26S proteasome-associated pad1 homolog		Theoretical pI = 6.06	TMW = 34577
CaOva3	34726	6.0	19	72
HL-60	34726	6.2	19	92
A-375	34726	6.1	24	120
Ubiquitin pathway				
Q9UBE0	Ubiquitin-like 1 activating enzyme E1A HSPC140		Theoretical pI = 5.17	TMW = 38450
SK_N_SH	38851	5.2	15	79
P61088	Ubiquitin-conjugating enzyme E2N		Theoretical pI = 6.13	TMW = 17138
Hela cervix	17184	6.0	11	102

(*continued*)

Table 2 (*continued*)

Cell line	Molecular weight	Observed pI	Peptides matched	Scores
Q92890	Ubiquitin fusion degradation protein 1 homolog		Theoretical pI = 5.96	TMW = 38725
A_549	34763	6.3	16	97
P09936	Ubiquitin carboxyl-terminal hydrolase isozyme L1		Theoretical pI = 5.33	TMW = 24824
A_549	25151	5.3	16	100
P45974	Ubiquitin carboxyl-terminal hydrolase 5		Theoretical pI = 4.91	TMW = 95786
A_549	94190	5.0	34	182
A_673	94190	5.1	25	118
Q9UHD9	Ubiquilin 2 62% similar to isoform of DA41 (human, acc.no: Q9H3R4)		Theoretical pI = 5.24	TMW = 65765
Saos-2	65655	5.6	12	63
Proteolytic enzymes/inhibitors				
Q13512	Protein B		Theoretical pI = 5.39	TMW = 62264
SK_N_SH	62796	6.0	19	89
CaOva3	62796	6.0	25	129
Q96KP4	Cytosolic nonspecific dipeptidase		Theoretical pI = 5.66	TMW = 52878
SK_N_SH	53161	5.8	14	82
P28838	Cytosol aminopeptidase		Theoretical pI = 6.29	TMW = 52640
A-375	53006	6.5	37	262
MCF-7	53006	6.6	26	151
Hela cervix	53006	6.8	25	154
P50579	Methionine aminopeptidase 2		Theoretical pI = 5.57	TMW = 52891
SK_N_SH	40488	5.6	12	79
HL-60	40488	5.7	13	89
P50453	Cytoplasmic antiproteinase 3		Theoretical pI = 5.61	TMW = 42403
Hela cervix	63227	6.5	25	143
P52888	Thimet oligopeptidase		Theoretical pI = 5.72	TMW = 78708
MCF-7	79571	6.4	26	147
	36531	5.9	23	176
P20807	Calpain 3		Theoretical pI = 5.81	TMW = 94253
A-375	94364	7.0	17	65
Q03154	Aminoacylase-1		Theoretical pI = 5.77	TMW = 45885
HCT116	46084	5.9	24	121
A-375	46084	5.9	38	267
MCF-7	46084	5.9	23	141
S65491	91% similar to isoform of 26S proteasome non-ATPase regulatory subunit 7 (acc.no.: P51665)		Theoretical pI = 6.29	TMW = 37025
A_673	36674	6.8	15	90
Hela cervix	36674	7.3	24	156
P09960	Leukotriene A-4 hydrolase		Theoretical pI = 5.80	TMW = 69154
MCF-7	69737	5.9	34	221
P30740	Leukocyte elastase inhibitor		Theoretical pI = 5.90	TMW = 42741
SK_N_SH	42829	5.9	9	61
HCT116	42829	6.0	17	121
A_549	42829	5.8	19	109
Hela cervix	42829	6.1	26	165
O75439	Mitochondrial processing peptidase beta subunit, mitochondrial (precursor)		Theoretical pI = 6.38	TMW = 54366
Saos-2	54875	6.0	14	68
SK_N_SH	54875	5.6	17	80
MCF-7	55073	6.0	26	155

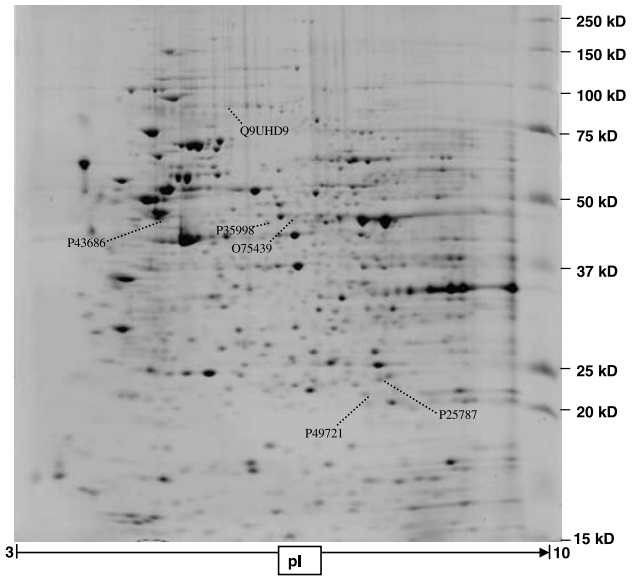

Fig. 1. 2-DE map of the human osteosarcoma cell line Saos-2. 2-DE was performed in an immobilized pI 3–10 nonlinear gradient strip, followed by the second-dimensional separation on 9–16% gradient polyacrylamide gels, and separated proteins were detected by colloidal Coomassie blue staining. The spots were analyzed by MALDI-MS or MS/MS. The identified proteins are designated by their SWISS-PROT accession number. The names of the proteins are listed in Table 2

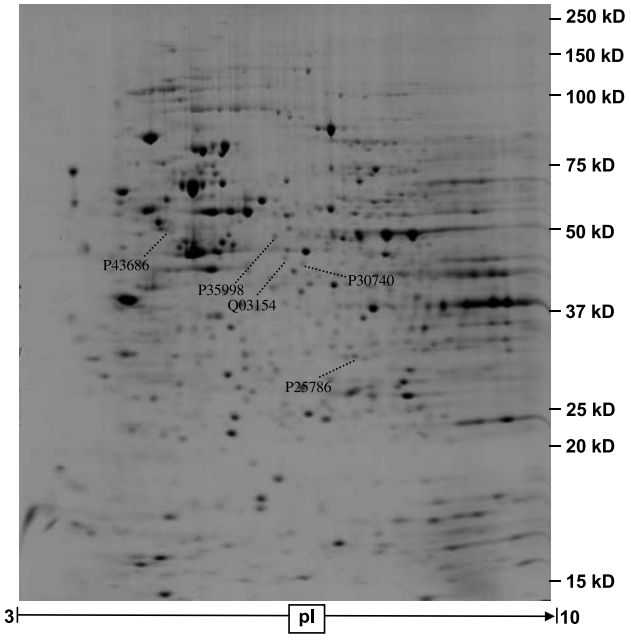

Fig. 3. 2-DE map of the human colorectal carcinoma cell line HCT-116. See legend Fig. 1 for details

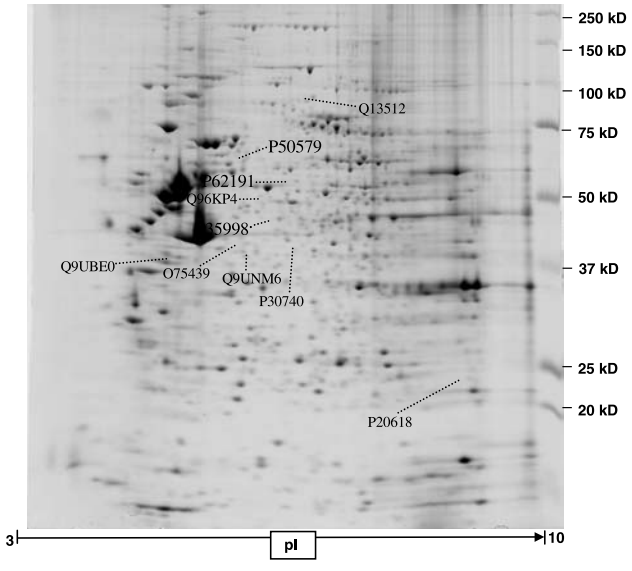

Fig. 2. 2-DE map of the human neuroblastoma cell line SK-N-SH. See legend Fig. 1 for details

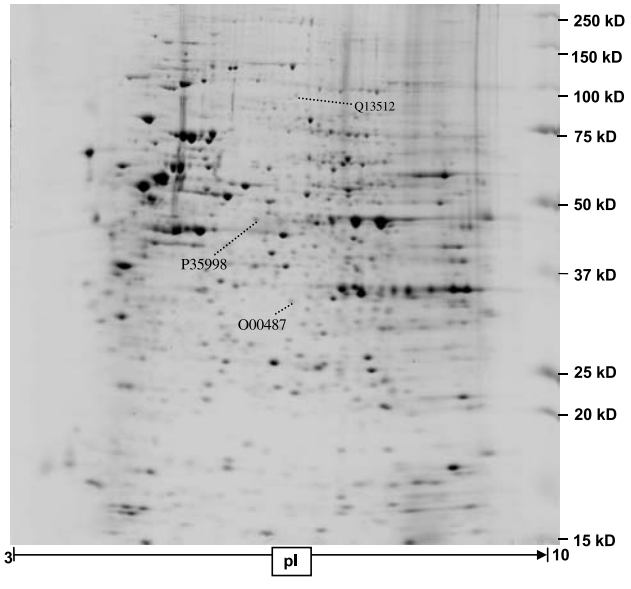

Fig. 4. 2-DE map of the human ovary adenocarcinoma cell line Caov3. See legend Fig. 1 for details

The 19S regulatory complex appears as a pan-like structure (base and lid) and forms a cap complex binding to both ends of the 20S proteasome. The base is able to degrade peptides and non-ubiquitylated proteins while the lid is required for ubiquitylated protein degradation providing the specificity of the complex. In addition, the 19S regulatory complex contributes to unfolding and linearizing proteins thus enabling entry of proteins into the catalytic inner core (Adams, 2004). Moreover, individual members of the 19S regulatory complex have been shown to be involved in regulation of transcription and DNA repair (Russell, 1999; Gonzalez et al., 2002). 11 components

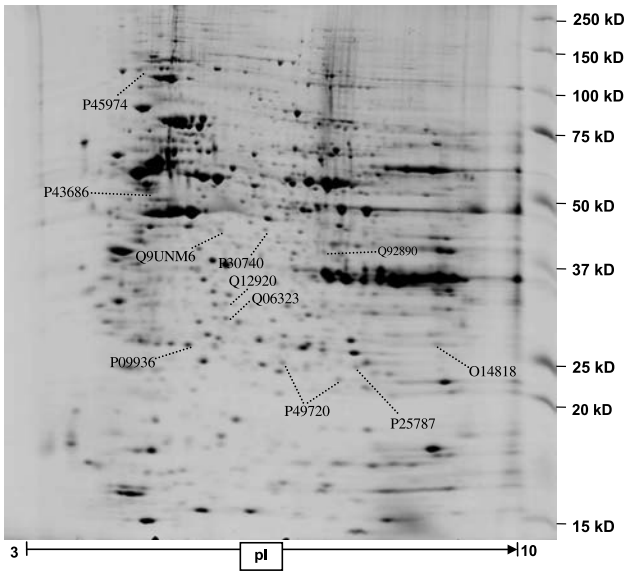

Fig. 5. 2-DE map of the human lung carcinoma cell line A-549. See legend Fig. 1 for details

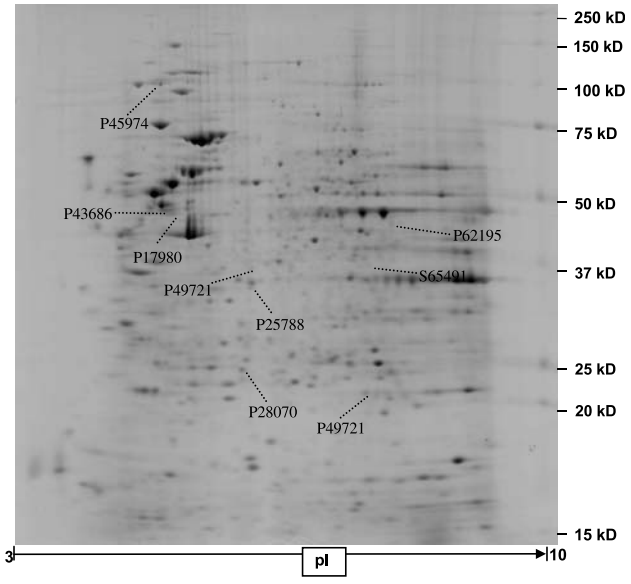

Fig. 7. 2-DE map of the human rhabdomyosarcoma cell line A-673. See legend Fig. 1 for details

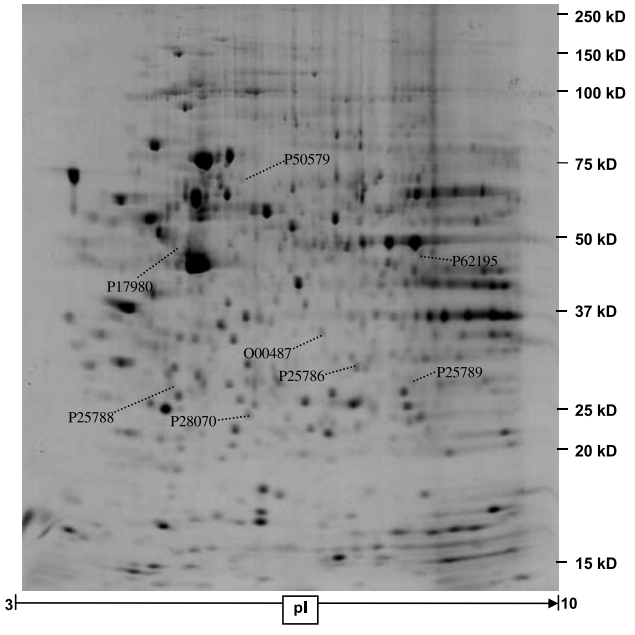

Fig. 6. 2-DE map of the human leukemia cell line HL-60. See legend Fig. 1 for details

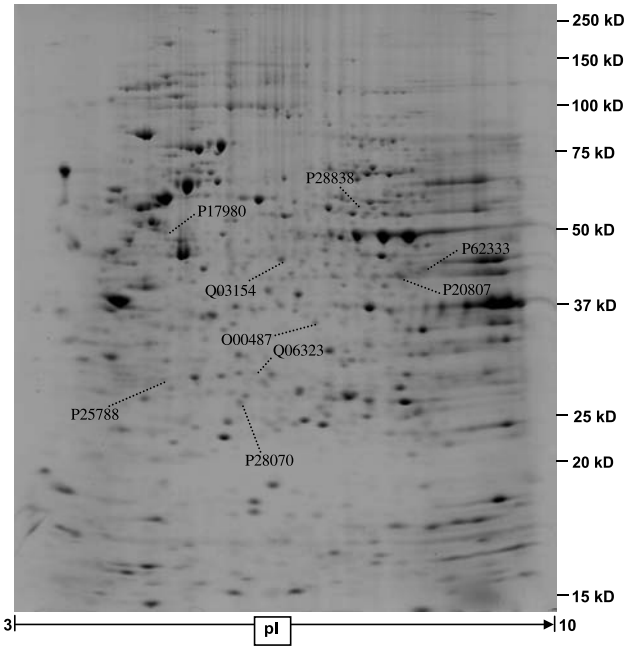

Fig. 8. 2-DE map of the human malignant melanoma cell line A-375. See legend Fig. 1 for details

were herein demonstrated: 26S protease regulatory subunit 4, 6a, 6b, 7, 8, S10B, 26S proteasome non-ATPase regulatory subunit 7, 10, 11, 13 and proteasome – associated pad1 homolog. All components presented with a single spot on 2 dimensional electrophoresis and observed pIs were comparable to predicted values except 26S proteasome non-ATPase regulatory subunit 7 in HeLa cells.

A couple of 19 regulatory complex components are of particular tumor biological relevance:

26S protease regulatory subunit 6a (syn.: TAT-binding protein-1; TBP-1), known to be involved in transcriptional regulation and playing a tentative role in cell proliferation, specifically interacts with tumor suppressor ARF (p14)

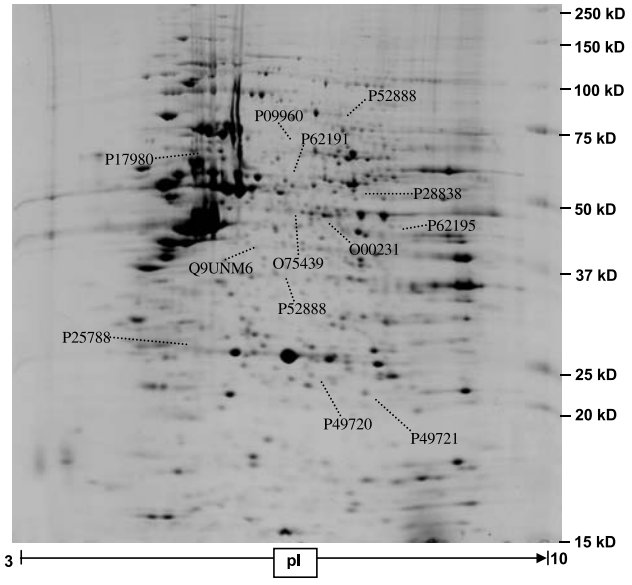

Fig. 9. 2-DE map of the human breast adenocarcinoma cell line MCF-7. See legend Fig. 1 for details

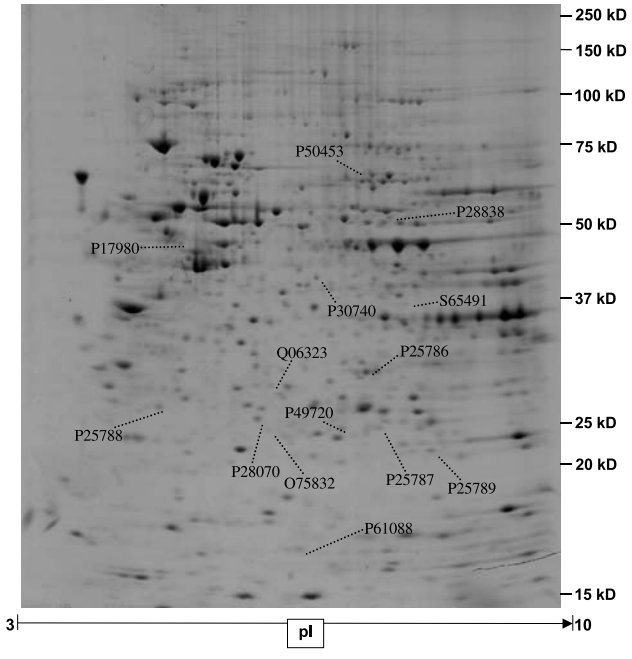

Fig. 10. 2-DE map of the human cervix adenocarcinoma cell line Hela. See legend Fig. 1 for details

that is frequently inactivated in human cancer. Binding of TBP-1 to ARF leads to increase of ARF levels with subsequent suppression of cell proliferation (Pollice et al., 2004). Here, TBP-1 was observed in leukemia, melanoma, rhabdomyosarcoma, breast and cervical cancer cell lines (Table 2).

26S protease regulatory subunit 7 (syn.: MSS1) is of interest as this structure was associated with cancer cachexia in tumor bearing rats (Combaret et al., 1999) and was detected in osteosarcoma, neuroblastoma, colorectal and ovarial carcinoma.

26S proteasome non-ATPase regulatory subunit 10 (syn.: gankyrin) is a recently discovered oncoprotein, overexpressed in most hepatocellular carcinomas (Sakurai et al., 2004). It induces growth and tumorigenicity in NIH/3T3 cells by destabilizing retinoblastoma protein RB1 (Higashitsuji et al., 2000) and therefore represents a major target for development of experimental strategies. Gankyrin was expressed exclusively in the HeLa cell line (Table 2).

26S proteasome-associated pad1 homolog (syn.: POH1/Rpn11) is a key proteasome-associated deubiquitinating enzyme. In fission yeast, overexpression of pad1 confers pleiotropic drug resistance by a pathway involving transcription factor AP1 (Spataro et al., 1997) and mammalian cells overexpressing POH1/Rpn11 display resistance to vinblastin, cisplatin and doxorubicin (Spataro et al., 2002). 26S proteasome-associated pad1 homolog may serve as a marker for multidrug resistant cells and was identified in ovarial carcinoma, leukemia and melanoma (Table 2).

The 11S regulator complex (syn.: PA28) is another regulatory complex associated with the 20S proteasome consisting of three subunits, alpha, beta, gamma. Binding of 11S regulator complex to 20S proteasome is not depending on ATP hydrolysis and – unlike the 19S regulatory subunit, the 11S regulator complex does not catalyse degradation of large proteins (Adams, 2004) but is responsible for MHC-class 1 antigen processing; that is greatly improved by interferon gamma induced expression of alpha and beta subunits (Kloetzel, 2004). The gamma subunit has been implicated in affecting proteasome-dependent signaling pathways modulating cell cycle control (Barton et al., 2004). A number of viral protein interactions with these proteasome subunits have been reported that may interfere with host anti-viral defense thereby contributing to mechanisms of cell transformation (Rivett and Hearn, 2004).

Two proteins, proteasome activator complex subunit 1 (PA28 alpha) and proteasome activator complex subunit 3 (PA28 gamma) were detected as single spots. pI values were calculated and were resembling predicted pIs. Proteasome activator complex subunit 3 was exclusively detected in the lung cancer cell line (Table 2).

Six proteins of the ubiquitin pathway, serving several functions were observed:

Ubiquitin-like 1 activating enzyme E1A, ubiquitin-conjugating enzyme E2N, ubiquitin fusion degradation 1 homolog, ubiquitin carboxyl-terminal hydrolase isozyme L1, ubiquitin carboxyl-terminal hydrolase 5 and ubiquilin 2. These structures were represented as single spots and the pI values were corresponding to the predicted pI.

Ubiquitin carboxyl-terminal hydrolase isozyme L1 (syn.: ubiquitin thiolesterase L1, PGP9.5, UCH-L1) is a de-ubiquitinating enzyme that has been linked to progression and differentiation of certain tumors (Maki et al., 1996; Liu et al., 2003). It was proposed as a marker for invasive colorectal cancer (Yamazaki et al., 2002) and was already detected in nearly all lung cancer lines (Bittencourt Rosas et al., 2001) including A549. We here confirm UCH-L1 expression in this cell lineage (Table 2, Fig. 5), the only out of ten cell lines studied. UCH-L1 inhibition as revealed by RNA-interference results into a proproliferative effect (Liu et al., 2003) although specific mechanisms of this response remain elusive.

Ubiquilin 2 (syn.: Chap1) is highly expressed in mitotic cells and increases the half-life of proteins destined to degradation by the proteasome. (SwissProt Accession Number: Q9UHD9). This protein was detectable in osteosarcoma only (Table 2).

No link to tumor biology has been described so far for the residual four ubiquitin pathway proteins.

Proteases are well known to be involved in cell migration, invasion, metastasis, angiogenesis and tumor surveillance.

The group of non-proteasomal-related proteases/inhibitors includes cytosolic nonspecific dipeptidase, cytosol aminopeptidase, methionine aminopeptidase 2, cytoplasmic antiproteinase 3, thimet oligopeptidase, calpain 3, aminoacylase 1, leukotriene A4 hydrolase, leucocyte elastase inhibitor, protein B and mitochondrial processing peptidase beta subunit.

These proteases were represented by single spots except thimet oligopeptidase that showed two expression forms. pI values deviated significantly from predicted values for mitochondrial processing peptidase beta subunit, cytoplasmic antiproteinase 3 and calpain 3 (Table 2).

Cytosol aminopeptidase (syn.: leucine aminopeptidase; LAP) is involved in cell migration and antigen presentation by trimming of the N-terminus of epitopes (Kloetzel and Ossendorp, 2004). LAP expression was associated with histological tumor grade in endometrial carcinoma (Kazeto et al., 2003) and was herein detectable in melanoma, breast cancer and HeLa cell lines (Table 2).

Methionine aminopeptidase 2 (MetAP2; syn.: p67) has been suggested as a novel target for cancer therapy as MetAP2 inhibition by the specific inhibitor A-357300 suppresses tumor growth through cell cycle arrest in the G(1) phase. Cytostasis was selectively induced in endothelial cells and in a subset of tumor cells shown in murine models of carcinoma, sarcoma and neuroblastoma (Wang et al., 2003). However, RNA interference studies failed to inhibit cell growth in human endothelial cells as well as in epithelial tumor cell lines (Kim et al., 2004). In the present study MetAP expression was demonstrated in neuroblastoma and leukemia (Table 2).

Cytoplasmic antiproteinase 3 (syn.: serpin B9, PI-9, granzyme B inhibitor) confers resistance to cytotoxic T-lymphocytes or natural killer cell killing by inactivation of granzyme B, the main effector of target-cell killing leading to destruction of the target cell by inducing apoptosis (Barrie et al., 2004). PI-9 enables tumor cells to escape this mechanism of immune defense and was observed in a variety of tumor cell lines (Medema et al., 2001). In contrast to this report, PI-9 was herein detectable in HeLa cells exclusively (Table 2).

Calpain 3 is able to specifically degrade tumor suppressor p27 and therefore involved in regulation of apoptosis and is one of genes highly expressed in melanoma (Weeraratna et al., 2004).

This observation at the transcriptional level could herewith be confirmed at the protein level: Calpain 3 was exclusively expressed in the melanoma cell line (Table 2).

Methodologically, MALDI-TOF-TOF with LIFT-technology fairly identified a series of proteasomal proteins and proteolytic systems independent of antibody availability and specificity. The method of two dimensional gel electrophoresis allowed concomitant demonstration and identification of several structures thus warranting the generation of individual cell line specific maps/patterns and indeed, the expressional patterns of individual cell lines vary enormously. Only high abundance proteins (i.e. spots visualized by Commassie staining) were detected as loading of higher protein amounts onto 2D gels would lead to decreased separation/resolution capacity. The fact that the method applied does not analyse hydrophobic, strongly acidic or strongly basic proteins (Lubec et al., 2003) is not a limiting factor as proteasomal proteins or proteases do not show these chemical properties.

4 Concluding remarks

A preliminary database and reference maps of proteasomal and proteolytic proteins in several tumor cell lines are reported and an analytical tool for the concomitant analysis is presented.

Given the pivotal importance of the ubiquitin – proteasome pathway we here aimed to identify a series of individual components that were already shown to be involved in tumor biological mechanisms and are representing major candidates and targets for development of new therapeutical strategies. Protein chemical rather than immunochemical identification as well as cell line specific expression of individual structures may assist to design studies in this area of research. We propose as next steps to generate complete maps of tumor and non-tumor cell lines by improving separation and detection by chemical prefractionation and subcellular compartmentalization.

Acknowledgements

We are highly indebted to the Red Bull Company, Salzburg, Austria, for generous financial support of the study.

The technical assistance of Kiseok Lee, MSc, is highly appreciated and secretarial work of Claudia Avramovic is appreciated.

We acknowledge contribution of the Österreichische Nationalbank (Project No: 9187) and the Forschungsgesellschaft für cerebrale Tumore.

References

Adams J (2004) The proteasome: a suitable antineoplastic target. Nat Rev Cancer 4: 349–360

Berndt P, Hobohm U, Langen H (1999) Reliable automatic protein identification from matrix-assisted laser desorption/ionization mass spectrometric peptide fingerprints. Electrophoresis 20: 3521–3526

Barrie MB, Stout HW, Abougergi MS, Miller BC, Thiele DL (2004) Antiviral cytokines induce hepatic expression of the granzyme B inhibitors, proteinase inhibitor 9 and serine proteinase inhibitor 6. J Immunol 172: 6453–6459

Barton LF, Runnels HA, Schell TD, Cho Y, Gibbson R, Tevethia SS, Deepe GS Jr, Monaco JJ (2004) Immune defects in 28-kDa proteasome activator gamma deficient mice. J Immunol 172: 3948–3954

Bittencourt Rosas SL, Caballero OL, Dong SM, da Costa Carvalho Mda G, Sidransky D, Jen J (2001) Methylation status in the promoter region of the human PGP9.5 gene in cancer and normal tissues. Cancer Lett 170: 73–79

Bradford MM (1976) A rapid and sensitive method for the quantitation of microgram quantities of protein utilizing the principle of protein-dye binding. Anal Biochem 72: 248–254

Chene P (2003) Inhibiting the p53-MDM2 interaction: an important target for cancer therapy. Nat Rev Cancer 3: 102–109

Combaret L, Ralliere C, Taillandier D, Tanaka K, Attair D (1999) Manipulation of the ubiquitin-proteasome pathway in cachexia: pentoxifylline suppresses the activation fo 20S and 26S in muscles from tumor-bearing rats. Mol Biol Rep 26: 95–101

Cusack JC Jr, Liu R, Houston M, Abendroth K, Elliott PJ, Adams J, Baldwin AS Jr (2001) Enhanced chemosensitivity to CPT-II with proteasome inhibitor PS-341: implicatons for systemci nuclear factor kappaB inhibition. Cancer Res 61: 3535–3540

Doherty FJ, Dawson S, Mayer RJ (2002) The ubiquitin-proteasome pathway of intracellular proteolysis. Essays Biochem 38: 51–63

Glotzer M, Murray AW, Kirschner MW (1991) Cyclin is degraded by the ubiquitin pathway. Nature 349: 132–138

Gonzalez F, Delahodde A, Kodadek T, Johnston SA (2002) Recruitment of a 19S proteasome subcomplex to an activated promoter. Science 296: 548–550

Higashitsuji H, Itoh K, Nagao T, Dawson S, Nonoguchi K, Kido T, Mayer RJ, Arii S, Fujita J (2000) Reduced stability of retinoblastoma protein by gankyrin, an oncogene andyrin-repeat protein overexpressed by hepatomas. Nat Med 6: 96–99

Jeremias I, Kupatt C, Baumann B, Herr I, Wirth T, Debatin KM (1998) Inhibition of nuclear factor kappaB activation attenuates apoptosis resistance in lymphoid cells. Blood 91: 4624–4631

Jesenberger V, Jentsch S (2002) Deadly encounter: ubiquitin meets apoptosis. Nat Rev Mol Cell Biol 3: 112–121

Karin M, Cao Y, Greten FR, Li ZW (2002) NF-kappaB in cancer: from innocent bystander to major culprit. Nat Rev Cancer 2: 301–310

Kazeto H, Nomura S, Ito N, Ito T, Watanabe Y, Kajiyama H, Shibata K, Ino K, Tamakoshi K, Hattori A, Kikkawa F, Nagasaka T, Tsujimoto M, Mizutani S (2003) Expression of adipocyte-derived leucine aminopeptidase in endometrial cancer. Association with tumor grade and CA-125. Tumour Biol 24: 203–208

Kim S, LaMontagne K, Sabio M, Sharma S, Versace RW, Yusuff N, Phillips PE (2004) Depletion of methionine aminopeptidase 2 does not alter cell response to fumagillin or bengamides. Cancer Res 64: 2984–2987

Kloetzel PM (2004) Generation of major histocompatibility complex class I antigens: functional interplay between proteasomes and TPPII. Nat Immunol 5: 661–669

Kloetzel PM, Ossendorp F (2004) Proteasome and peptidase function in MHC-class-I-mediated antigen presentation. Curr Opin Immunol 16: 76–81

Liu Y, Lashuel HA, Choi S, Xing X, Case A, Ni J, Yeh LA, Cuny GD, Stein RL, Lansbury PT Jr (2003) Discovery of inhibitors that elucidate the role of UCH-L1 activity in the H1299 lung cancer cell line. Chem Biol 10: 837–846

Lubec G, Krapfenbauer K, Fountoulakis M (2003) Proteomics in brain research: potentials and limitations. Prog Neurobiol 69: 193–211

Maki A, Mohammad RM, Smith M, Al-Katib A (1996) Role of ubiquitin carboxyl terminal hydrolase in the differentiation of human acute lymphoblastic leukemia cell line, Reh. Differentiation 60: 59–66

Medema JP, de Jong J, Peltenburg LT, Verdegaal EM, Gorter A, Bres SA, Franken KL, Hahne M, Albar JP, Melief CJ, Offringa R (2001) Blockade of the granzyme B/perforin pathway through overexpression of the serine protease inhibitor PI-9/SPI-6 constitutes a mechanism for immune escape by tumors. Proc Natl Acad Sci USA 98: 11515–11520

Ohta T, Fukuda M (2004) Ubiquitin and breast cancer. Oncogene 23: 2079–2088

Pollice A, Nasti V, Ronca R, Vivo M, Lo Iacono M, Calogero R, Calabro V, La Montia G (2004) Functional and physical interaction of the human tumor surpressor with Tat-binding protein-1. J Biol Chem 279: 6345–6353

Rivett AJ, Hearn AR (2004) Proteasome function in antigen presentation: immunoproteasome complexes, peptide production, and interactions with viral proteins. Curr Protein Pept Sci 5: 153–161

Russell SJ, Reed SH, Huang W, Friedberg EC, Johnston SA (1999) The 19S regulatory complex f the proteasome functions independently of proteolysis in nucleotide excision repair. Mol Cell 3: 687–695

Sakamoto KM (2002) Ubiquitin-dependent proteolysis: its role in human diseases and the design of therapeutic strategies. Mol Genet Metab 77: 44–56

Sakurai T, Itoh K, Higashitsuji H, Nagao T, Nonoguchi K, Chiba T, Fujita T (2004) A cleaved form of MAGE-A4 binds to Miz-I and induces apoptosis in human cells. J Biol Chem 279: 15505–15514

Spataro V, Toda T, Craig R, Seeger M, Dubiel W, Harris AL, Norbury C (1997) Resistance to diverse drug and ultraviolet light conferred by overexpression of a novel human 26S proteasome unit. J Biol Chem 272: 30470–30475

Spataro V, Simmen K, Realini CA (2002) The essential 26S proteasome subunit Rpn II confers multidrug resistance to mammalian cells. Anticancer Res 22: 3905–3909

Suckau D, Resemann A, Schuerenberg M, Hufnagel P, Franzen J, Holle A (2003) A novel MALDI LIFT-TOF/TOF mass spectrometer for proteomics. Anal Bioanal Chem 376: 952–965

Wang CY, Cusack JC Jr, Liu R, Baldwin AS Jr (1999) Control of inducible chemoresistance: enhanced anti-tumor therapy through increased apoptosis by inhibition of NFkappaB. Nat Med 5: 412–417

Wang J, Sheppard GS, Lou P, Kawai M, BaMaung N, Erickson SA, Tucker-Garcia L, Park C, Bouska J, Wang YC, Frost D, Tapang P, Albert DH, Morgan SJ, Morowitz M, Shusterman S, Maris JM, Lesniewski R, Henkin J (2003) Tumor suppression by a rationally designed reversible inhibitor of methionine aminopeptidase-2. Cancer Res 63: 7861–7869

Weeraratna AT, Becker D, Carr KM, Duray PH, Rosenblatt KP, Yang S, Chen Y, Bittner M, Strausberg RL, Riggins GJ, Wagner U, Kallioniemi OP, Trent JM, Morin PJ, Meltzer PS (2004) Generation and analysis of melanoma SAGE libraries: SAGE advice on the melanoma transcriptome. Oncogene 23: 2264–2274

Weitzdoerfer R, Fountoulakis M, Lubec G (2002) Reduction of actin-related protein complex 2/3 in fetal Down sydrome brain. Biochem Biophys Res Commun 293: 836–841

Yamazaki T, Hibi K, Takase T, Tezel E, Nakayama H, Kasai Y, Ito K, Akiyana S, Nagasaka T, Nakao A (2002) PGP9.5 as a marker for invasive colorectal cancer. Clin Cancer Res 8: 192–195

Yang JW, Czech T, Lubec G (2004) Proteomic profiling of human hippocampus. Electrophoresis 25: 1169–1174

Yang Y, Li CC, Weissman AM (2004) Regulating the p53 system through ubiquitination. Oncogene 23: 2096–2106

Authors' address: Prof. Dr. Gert Lubec, CChem, FRSC (UK), Department of Pediatrics, Division of Basic Sciences, Universtiy of Vienna, Waehringer Guertel 18-20, 1090 Vienna, Austria,
Fax: + 43-1-40400-3194, E-mail: gert.lubec@meduniwien.ac.at